Phenotypic differences between interfertile *Chlamydomonas* species

We're crossing *C. reinhardtii* and *C. smithii* algae for high-throughput genotype-phenotype mapping. In preparation, we're comparing the parents to uncover unique species-specific phenotypes.

Version 4, published Sep 28, 2023. Originally published Jun 22, 2023.

Arcadia Science DOI: 10.57844/arcadia-35f0-3e16

Purpose

We're working to understand the associations between genotypes and phenotypes across the tree of life. Analyzing variation among interbreeding populations is a powerful tool for dissecting genotype-phenotype relationships.

To build our framework from the bottom up, we're starting by breeding interfertile *Chlamydomonas* species — *C. reinhardtii* and *C. smithii* — and performing high-dimensional characterization of many aspects of their biology. Here, we describe various phenotypes for each of the two parental species. These phenotypes will serve as a baseline against which we will compare phenotypic and genotypic differences in the progeny of the hybridized strains.

So far, we've studied the two species' growth on various types of media, sensitivity to lysis by detergent, and morphologies. We expect to have data on their motility, chloroplast fluorescence decay, and organelle morphologies in the near future. We're sharing the data as we collect and analyze it, and expect to add new phenotypic data over time. We hope that readers working with these species will find it useful to have access to our findings as soon as we're able to describe them.

- This pub is part of the **platform effort**, "Genetics: Decoding evolutionary drivers across biology." Visit the platform narrative for more background and

context.

- Our **Fiji macro**, **Cellprofiler pipeline**, and **code** in R and Python are available in this GitHub repository.

Background and goals

We are advancing an initiative to understand how genes and environments interact to drive variation in organismal traits. To investigate the relationship between genotypes and phenotypes, we need a population with both genetic and phenotypic diversity. A traditional solution would be to perform mutagenesis in an otherwise isogenic population, and then isolate individual alleles. While useful, the genetic changes that result from mutagenesis are fundamentally different from the forms of genetic variation that drive phenotypic variation in an actively interbreeding natural population. Such an approach also won't allow us to look at variation driven by specific allele combinations. A powerful alternative is to study the relationship between genotypic and phenotypic variation within a naturally varying population, as is done with experiments such as quantitative trait locus (QTL) mapping [1].

We chose to create a diverse population by hybridizing two interfertile species. We selected *Chlamydomonas reinhardtii* and *Chlamydomonas smithii* because they produce viable progeny when mated [2][3], are easy to maintain in clonal cultures, and, being unicellular algae, offer the potential to perform a variety of high-throughput analyses. However, little is known about the aspects of biology that differentiate these species (see Table 1). Given this, we are comparing a variety of phenotypes among these parent species to identify key axes of variation between them. These analyses will act as priors for all downstream comparisons of their progeny.

Brief background on *Chlamydomonas reinhardtii* and *smithii* species

C. reinhardtii is widely used as a model to study cellular processes like photosynthesis, cilia formation, and cell division [4]. *C. smithii* is less well characterized, even though these two species share a similar history [5][6]. In fact,

the cells we used in this study were propagated from cultures isolated from soil fields in Massachusetts in 1945. For more than seven decades, both species have been subcultured under laboratory conditions, implying that any apparent differences between the species shouldn't stem from disparate lab adaptations, since they have been exposed to similar levels of adaptation opportunities.

To date, several genotypic differences have been observed between these two species including differences in their nuclear, chloroplast, and mitochondrial genomes [7][8][9][10][11], but a quality reference genome for *C. smithii* does not yet exist. Phenotypic differences are less well characterized — we've summarized the few previously reported differences in Table 1. The dearth of studies on *C. smithii* has led some to mischaracterize the species as a wild-type *C. reinhardtii* strain. For instance, *C. smithii* was recently used as a baseline wild-type *C. reinhardtii* strain in a comparison with *C. reinhardtii* cell wall mutants [12] and has been referred to as a *C. reinhardtii* field strain even though it has been subcultured in labs for the same amount of time as bona fide *C. reinhardtii* lab strains [7].

Phenotype	***C. reinhardtii***	***C. smithii***
Doubling time in the dark [13]	~24–31 hours	~72–108 hours
Cell volume [13]	110–115 μm^3	100 μm^3
Nuclear volume [13]	9.5–10.3 μm^3	11 μm^3
Morphology	10 µm long [14] 3 µm wide [14] ~6.5 um diameter [7]	7.5–11 µm long [3] 3–7.5 µm wide [3] ~7.5 um diameter [7]
Chlorophyll content [7]	~1600–2100 APC-A intensity	~1800 APC-A intensity
Heterotrophic growth [7]	~0.09-0.27 omnilog units	~0.92 omnilog units
Phototrophic growth [7]	—	~0.003 ΔOD_{680}/h

Table 1. **Previously reported phenotypic differences between the two *Chlamydomonas* species we're studying**.

The approach

Before isolating *C. reinhardtii* × *C. smithii* hybrid strains, it is important that we understand the baseline differences between these two species. We are

investigating specific traits in these organisms that we can efficiently adapt to high-throughput methods, align with our research goals, and which take advantage of our in-house tools and expertise. We're using both single-cell and multi-cell analyses to differentiate these species. These findings will provide the foundation for upcoming experiments to map associations between genotypes and phenotypes.

Here, we describe the first three sets of phenotypes that we observed between these two *Chlamydomonas* species. First, we observed their growth under various culture conditions, altering nutrients, illumination, and temperature. We used two *C. reinhardtii* strains of opposing mating types in this initial study to determine if these phenotypes were mating-type dependent; however, we only used one *C. smithii* strain because a mating type pair of this species is not yet accessible through culture collection centers. We chose which growth media to use in this study based on in-house availability and variability of nutrients. Next, we treated cells with a low-concentration detergent to test resistance to lysis. Finally, we did a thorough analysis of the two-dimensional morphology of the two *Chlamydomonas* species. We'll add additional phenotypes to this pub as we generate the data.

Species and strains

Species	Strain numbers and source links	Mating type	Site of parent isolation
Chlamydomonas reinhardtii	137c, cc-124, UTEX2243, SAG 33.89 (source)	(−)	• Amherst, Massachusetts, USA • Potato field soil • 1945
Chlamydomonas reinhardtii	137c, cc-125, UTEX2244, SAG 34.89 (source)	(+)	• Amherst, Massachusetts, USA • Potato field soil • 1945
Chlamydomonas smithii	136f, cc-1373, UTEX1062, SAG 54.72 (source)	(+)	• South Deerfield, Massachusetts, USA • Tobacco field soil • 1945

Table 2. **Organisms used in this pub**.

We ordered all species from the Chlamydomonas Resource Center.

Cell maintenance

After receiving strains from the culture center (Table 2), we streaked cells out to individual colonies on TAP media with 1.5% agar. We cultured cells from single colonies in liquid TAP media (UTEX) and then seeded them onto plates of TAP media with 1.5% agar to form a confluent lawn either at 24 °C under constant illumination or at ambient temperature under 12:12-hour light:dark cycles. For the 24 °C condition, we maintained cells in an incubator (internal dimensions 84 × 46 × 33 cm) equipped with five dimmable LED strips emitting across the red and blue spectrum (460 nm – 620 nm). Our light meter read the luminosity ranging from 500–3,300 lux in this enclosed environment. We grew cells at ambient temperature on an open bench equipped with three GE Full Balanced Spectrum 9 Watt BR30 LED bulbs installed in clamp lamps. Our light meter read the luminosity at 1,400–2,500 lux in this area.

Extracting data displayed in Table 1

For the chlorophyll content, heterotrophic growth, and phototrophic growth data in Table 1, we extracted raw values from published bar graphs [7] using the WebPlotDigitizer tool [15].

Media components

We made all solid media with 1.5% agar. We made "water" plates with ultrapure water from a Milli-Q EQ 7008 system equipped with a 0.22 µm filter. Individual media components are as follows:

TAP (tris-acetate-phosphate) media

375 µM NH_4Cl, 17.5 µM $CaCl_2*2H_2O$, 20 µM $MgSO_4*7H_2O$, 6 µM Na_2HPO_4, 4 µM KH_2PO_4, 200 µM Trizma base, 170 µM glacial acetic acid, 0.1% v/v of Hunter's trace elements solution (134 µM $Na_2EDTA*2H_2O$, 770 µM $ZnSO_4*7H_2O$, 184 µM H_3BO_3, 26 µM $MnCl_2*4H_2O$, 18 µM $FeSO_4*7H_2O$, 7 µM $CoCl_2*6H_2O$, 5 µM $CuSO_4*5H_2O$, and 800 nM $(NH_4)_6Mo_7O_{24}*4H_2O$). Suspended in ultrapure water. We purchased complete liquid media from UTEX.

Soil extract media

96% Bristol media and 4% pasteurized soil water supernatant (0.05 mM $CaCO_3$, 2.5% greenhouse soil, suspended in ultrapure water). We purchased complete liquid media from UTEX.

Bristol media

2.94 mM $NaNO_3$, 0.17 mM $CaCl_2*2H_2O$, 0.3 mM $MgSO_4*7H_2O$, 0.43 mM K_2HPO_4, 1.29 mM KH_2PO_4, and 0.43 mM NaCl. Suspended in ultrapure fresh water. We purchased complete liquid media from UTEX.

Kuhl's media

10 mM KNO_3, 4.5 mM $NaH_2PO_4*H_2O$, 0.5 mM $Na_2HPO_4*2H_2O$, 1 mM $MgSO_4*7H_2O$, 0.1 mM $CaCl_3*2H_2O$, 24.8 µM $FeSO_4*7H_2O$, 25 µM Na_2EDTA, 987 nM

H_3BO_3, 1 µM $MnSO_4*H_2O$, 1 µM $ZnSO_4*7H_2O$, 10 nM $CuSO_4*5H_2O$, 10 nM $(NH_4)_6Mo_7O_{24}*4H_2O$. Suspended in ultrapure water.

K media

882 µM $NaNO_3$, 50 µM NH_4Cl, 10 µM Na_2 b-glycerophosphate, 504 µM $Na_2SiO_3*9H_2O$, 10 nM H_2SeO_3, 1 mM tris base (pH 7.2), 111 µM $Na_2EDTA*2H_2O$, 12 µM $FeCl_3*6H_2O$, 900 nM $MnCl_2*4H_2O$, 80 nM $ZnSO_4*7H_2O$, 42 nM $CoCl_2*6H_2O$, 26 nM $Na_2MoO_4*2H_2O$, 10 nM $CuSO_4*5H_2O$, 296 nM thiamine HCl, 0.21 nM biotin, and 0.04 nM cyanocobalamin. Suspended in filtered synthetic seawater (described below). We purchased a K media kit from the NCMA at Bigelow Labs.

F/2 media

880 µM $NaNO_3$, 36 µM $NaH_2PO_4*H_2O$, 106 µM $Na_2SiO_3*9H_2O$, 11.7 nM $Na_2EDTA*2H_2O$, 11.7 nM $Fe(NH_4)_2(SO_4)_2*6H_2O$, 0.9 nM $MnSO_4*H_2O$, 0.08 nM $ZnSO_4*7H_2O$, 0.05 nM $CoSO_4*7H_2O$, 0.04 nM $CuCl_2*2H_2O$, 0.03 nM $Na_2MoO_4*2H_2O$, 100 nM cyanocobalamin, 126 µM thiamine, and 100 nM biotin. Suspended in pasteurized seawater. We purchased complete liquid media from UTEX.

F/2 − Si media

882 µM $NaNO_3$, 36.8 µM NaH_2PO_4, 11.7 µM $Na_2EDTA*2H_2O$, 11.6 µM $FeCl_3*6H_2O$, 909 nM $MnCl_2*_4H_2O$, 76 nM $ZnSO_4*7H_2O$, 42 nM $CoCl_2*2H_2O$, 40 nM $CuSO_4*5H_2O$, 25 nM $Na_2MoO_4*2H_2O$, 20.5 nM biotin, 4 nM cyanocobalamin, and 296 nM thiamine. We purchased liquid media from Sigma-Aldrich (G0154) at 50× concentration and diluted to 1× in filtered synthetic seawater (described below).

Synthetic seawater [RICCA Chemical Company: R8363000]

409 mM NaCl, 53 mM $MgCl_2*6H_2O$, 28 mM Na_2SO_4, 10 mM $CaCl_2*2H_2O$, 1 mM KCl, 1 mM $NaHCO_3$, 1 mM KBr, 0.4 mM $SrCl_2*6H_2O$, 1 mM H_3BO_3, 3 mM NaOH, and 2 mM NaF. Suspended in ultrapure water.

Erdschreiber's media

2.3 mM $NaNO_3$, 67 µM Na_2HPO_4*$7H_2O$, 23.7 µM Na_2EDTA*$2H_2O$, 4.3 µM $FeCl_3$*$6H_2O$, 2.5 µM $MnCl_2$*$4H_2O$, 400 nM $ZnCl_2$, 100 nM $CoCl_2$*$6H_2O$, 200 nM Na_2MoO_4*$2H_2O$, 100 nM cyanocobalamin, and 50 µM HEPES. Suspended in pasteurized seawater. For every 1 L of media, the supplier adds 50 mL of "Soil Water: GR+ Medium" (0.05 mM CaCO3, 2.5% greenhouse soil, suspended in ultrapure water). We purchased complete liquid media from UTEX.

L1 media in marine broth (MB + L1)

882 µM $NaNO_3$, 36.2 µM NaH2PO_4*H_2O, 106 µM Na_2SiO_3*$9H_2O$, 11.7 µM Na_2EDTA *$2H_2O$, 11.7 µM $FeCl_3$*$6H_2O$, 900 nM $MnCl_2$*$4H_2O$, 80 nM $ZnSO_4$*$7H_2O$, 50 nM $CoCl_2$*$6H_2O$, 10 nM $CuSO_4$*$5H_2O$, 8.22 nM Na_2MoO_4*$2H_2O$, 10 nM H_2SeO_3, 10 nM Na_3VO_4, 10 nM K_2CrO_4, 296 nM thiamine HCl, 0.21 nM biotin, and 0.04 nM cyanocobalamin. Suspended in marine broth 2216 [5 g/L peptone, 1 g/L yeast extract, 0.41 mM $C_6H_5FeO_7$, 333.1 mM NaCl, 62 mM $MgCl_2$, 26.9 mM $MgSO_4$, 16.2 mM $CaCl_2$, 7.4 mM KCl, 1.9 mM $NaHCO_3$, 0.67 mM KBr, 0.21 mM $SrCl_2$, 0.36 mM H_3BO_3, 0.033 mM Na_2SiO_3, 0.06 mM NaF, 0.02 mM NH_4NO_3, and 0.056 mM Na_2HPO_4 in ultrapure water.] We purchased an L1 media kit from the NCMA at Bigelow Labs. In this instance, we suspended L1 in marine broth 2216 instead of synthetic seawater because autoclaving synthetic seawater often results in nutrients precipitating out **[16]** and the addition of peptone increases the media's buffer capacity, preventing excessive precipitation **[17]**.

Spot assays

We maintained cells on plates of TAP media with 1.5% agar under a 12/12-hr light-dark cycle at ambient temperature. One day prior to experimentation, we seeded cells in 3 mL of liquid TAP media or sterile water and grew them at ambient temperature under a 12/12-hr light-dark cycle while rotating at 46 rpm at a ~120° angle in a rotator drum. The next day, we measured the optical density at 730 nm for each strain using a SpectraMax iD3 plate reader (Molecular Devices). We diluted dense cultures to have equal concentrations of cells. We conducted a serial dilution of the samples, following a progressive pattern of (1:1, 1:2, 1:4, 1:8, 1:16) to gradually reduce the concentration at each successive step in either water or TAP. We spotted samples grown under each condition onto nine agar plates per growth medium in 10 µL volumes. We kept plates at ambient temperature overnight to allow spots to dry.

The next day, we flipped and sealed plates. We then grew three plates from each group at 17 °C or ambient temperature under a 12/12-hr light-dark cycle or at 24 °C under constant illumination. For the 17 °C condition, we grew cells in an incubator (internal dimensions 28 × 25 × 36 cm) equipped with three dimmable LED strips (48 LEDs/strip) emitting the full spectrum of visible light. Our light meter read the luminosity at 1,800 lux in this enclosed environment. We allowed cells to grow for 16–40 days, depending on the initial cell concentration, and then imaged the plates using an Azure 600 imaging system (Azure Biosystems) under "true color imaging" settings.

Detergent treatment

We grew cells in liquid TAP media for 10 days while shaking under a 12/12-hour light-dark cycle at ambient temperature. On the day of the experiment, we measured the OD_{730} of each species to confirm similar cell densities. We collected cells for each reaction through centrifugation at 3,500 × g for five minutes and then resuspended the cells in 100 uL of reaction buffer (20 mM Tris-HCl; 5 mM $CaCl_2$; 5 mM $MgCl_2$). We next added an equal volume of 0.1% Triton X-100 (bringing its final concentration to 0.05%) to treated cells or an equal volume of reaction buffer to control cells. We vortexed all cells for one minute using the Scientific Industries Disruptor Genie at 3,000 rpm. We immediately collected cells by centrifugation at 13,000 × g for five minutes. We transferred 100 µL of supernatant from each reaction across a 96-well plate and measured the OD_{435} using a Molecular Devices SpectraMax ID3 plate reader (Absorption, Endpoint, Lm1: 435 nm; PathCheck: On; Detection Method: Precise; Shake Before: 00:05 [high intensity]). We subtracted the OD_{435} of reaction buffer or reaction buffer with 0.05% Triton X-100 from each measurement. We performed statistical analyses using GraphPad Prism. Briefly, we tested for normality using a Shapiro-Wilk test, which revealed that the distribution of untreated *C. reinhardtii* (+) was not normal. We performed the non-parametric ANOVA (Kruskal–Wallis test) and Dunn's multiple comparisons test. The post-hoc test adjusts for multiple comparisons, controlling for type I errors (at 0.05). Asterisks in figures indicate the adjusted p values as follows: *p < 0.05, ns means not significant.

Microscopy

Sample prep: Media-dependent morphologies (Figure 5, Video 1, Video 2)

We grew cells on 1.5% agar in the indicated media. We picked individual colonies with a sterile loop and suspended them in sterile water, placed in a 96-well plate with a #1.5 glass coverslip, and imaged immediately. For Video 1 and Video 2, we suspended cells in L1 media and plated on an Arralyze glass coverslip with 400 μm flat-bottom wells. We mounted coverslips on a standard microscope slide and sealed with VALAP (1:1:1 mixture of Vaseline, lanolin, and paraffin wax).

Sample prep: Gamete enrichment for morphology measurements

We scooped cells from agar plates growing either *C. reinhardtii* or *C. smithii* using a sterile loop and deposited them into 100 μl of water. We scooped approximately 1 cm^2 from a lawn of cells. We left the cells on the benchtop overnight (16–20 hours). This incubation step promotes gamete formation. Clumps of cells and immotile cells settle to the bottom, and motile cells are enriched in the supernatant. We loaded cells from the supernatant onto agar microchambers **[18]** immediately before imaging. We mounted and imaged *C. smithii* and then *C. reinhardtii*. We performed the procedure four times on different days with cells obtained from the same lawn plates (Figure 7). We created the agar microchambers and loaded the cells according to a standardized protocol, aiming to load 1–3 cells per well **[19]**.

Imaging: Media-dependent morphologies (Figure 5, Video 1, Video 2)

We acquired micrographs with a Yokogawa CSU W1-SoRa scanner unit attached to a Nikon Ti2-E confocal microscope set up with a LIDA Light Engine for RGB color images. We used a Plan Apo λ 60× oil objective with a 1.5× magnifier or a Plan Apo λ 10× air objective. We processed all imaging data using FIJI software (NIH). We used the StackReg Fiji plugin from the BIG-EPFL package to correct for sample drift during extended time-lapse imaging **[20]**.

Imaging: Morphology experiment (Figure 7)

We collected videos on a Nikon Ti2-E microscope equipped with a Photometrics Kinetix digital scMos camera. We performed differential interference contrast (DIC) imaging using a Plan Apo 10× 0.45 Air objective. We collected videos with a 5.1 ms exposure with acquisition every 50 ms for three minutes. We placed a red light

filter [IR longpass, 610 nm (ThorLabs)] in the light path to maintain swimming behavior of cells [21].

Image processing and cell morphology analysis

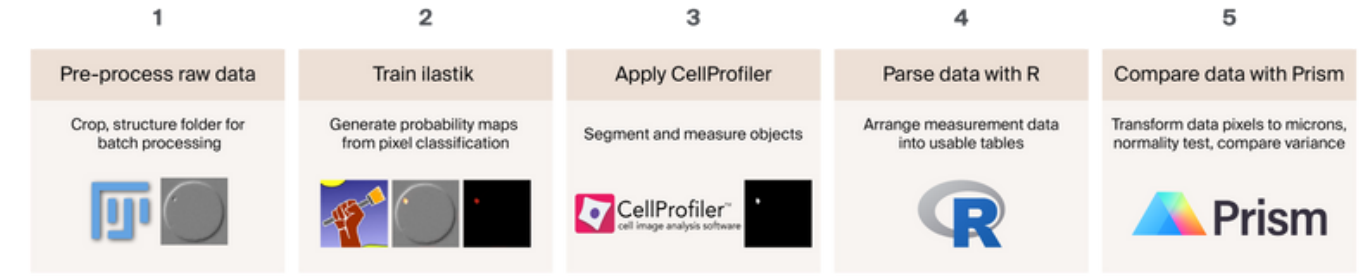

Figure 1. **Visual overview of our image processing and analysis workflow**.
We performed regression analyses and generated violin plots in R and used Prism for scatter plots.

Pre-processing

We cropped individual microchambers using an interactive Fiji macro in batch [22]. We applied the pixel classifier to the first 100 frames (five seconds of video) of each three-minute video to generate probability maps in batch. We determined which frames were in focus by first calculating the second derivative of each frame. Then we calculated the variance of those values within each frame. When you plot these values from the first frame to the last (frame 3600), there are peaks and valleys in the plot. We selected the frame that corresponded to each peak (the local maximum) and then took the three frames before and after that particular frame.

Training

We trained a pixel classifier to distinguish cells from background in ilastik [23]. We performed training on a subset of images of 3,600 frames of the three-minute videos. The training subset consisted of every 60th frame in the videos, approximately 2% of the total frames. We used the automatically suggested features in ilastik for the pixel classification. We also testedapplying the pixel classifier to a subset of images of cells in focus. We determined which frames

were in focus by identifying frames with local maxima of the variance of the second derivative (variance of the Laplacian [24]) of the images relative to adjacent frames. We performed training on all of the microchambers to ensure that we captured the full diversity of images in our experimental replicates. We segmented objects (i.e. cells) using a probability cutoff of 50% with a size range between 5–40 pixels in CellProfiler [25]. The probability cutoff was chosen based on a qualitative visual inspection of the segmentation. We determined the size cutoff by measuring cells in CellProfiler and adding a 10 pixel buffer on both ends of the size range. We then collected measurements of the objects using CellProfiler. We compiled spreadsheets of the measurements and parsed the data for comparative analysis using R scripts.

Analyses

We generated the plots of empirical measures and performed statistical analyses using GraphPad Prism because of our familiarity with the program, but others can run these analyses in R. Briefly, we transformed the data from pixels to microns, tested for outliers to clean the data [ROUT (Q = 1%)], and then tested for normality (D'Agostino & Pearson test, Anderson-Darling test, Shapiro-Wilk test, and Kolmogorov-Smirnov test). If data were distributed normally, we partitioned the variance by doing a one-way ANOVA and Tukey's multiple comparison test to determine the treatments that differed from one another. If the data were not normal, we performed the non-parametric equivalent, a Kruskal-Wallis test and Dunn's multiple comparisons test. In both cases, the post-hoc tests adjust for multiple comparisons, controlling for type I errors (at 0.05). Asterisks in figures indicate the adjusted p values as follows: *$p < 0.05$, **$p < 0.01$, ***$p < 0.001$, and ****$p < 0.0001$. ns means not significant.

Given potential experiment-level variability, we used a linear regression to remove the effect of experiment on area and analyzed the residuals. We compared the residuals using a Kruskal-Wallis test followed by a Bonferroni correction (Supplemental Figure 3).

Average cell modeling

We used ChatGPT to write Python code to visualize a cell of average size and shape based on our empirical mean and standard deviation measurements. We

generated SVG files that we stylized in Adobe Illustrator (Figure 7, D). We also used ChatGPT to comment this code.

> The **Fiji macro**, **Cellprofiler pipeline**, and **code** in R and Python are available in this GitHub repository (DOI: 10.5281/zenodo.8187999).

Writing

We used ChatGPT to suggest wording ideas and streamline/clarify content, and then edited the AI-generated text.

The results

Growth on various media

We decided to try growing both *Chlamydomonas* species on a variety of media to see if we could identify any obvious growth differences. In this initial study, we included two *C. reinhardtii* strains of opposite mating types to ensure any observed phenotypic differences aren't mating-type dependent or strain-specific.

We can maintain both *C. reinhardtii* and *C. smithii* in standard TAP (tris-acetate-phosphate) media [13]. However, we were surprised to see *C. smithii* outgrowing *C. reinhardtii* on other Chlorophyceae (green algae) media — soil extract media and Bristol media (Figure 2). The few *C. reinhardtii* colonies we did see looked more yellow than the usual green, a sign of chlorosis, which is consistent with poor nutrition [26]. Bristol media is richer than TAP media in several components, including nitrogen, phosphate, and multiple salt ions, including Mg^{2+}, Na^{+}, K^{+}, but lacks the trace heavy metals found in TAP media. Soil extract media is Bristol media supplemented with 4% pasteurized soil, which likely contains trace metals similar to TAP media, suggesting *C. smithii* is more adaptable to high-nutrient media than *C. reinhardtii*.

The temperature and illumination conditions we tested (Supplemental Figure 1, Supplemental Figure 2) had no obvious impact on colony growth, except visible colonies started to appear quicker under constant illumination in a controlled 24 °C environment, consistent with previous work [27]. We therefore decided to test just those growth conditions going forward.

Both species displayed slow growth on potassium nitrate-based Kuhl's media, though *C. smithii* grew slightly better. Surprisingly, we observed *C. smithii* growing on plates consisting of 1.5% agar in only ultrapure Milli-Q filtered water, even though we washed cells three times in ultrapure water prior to plating to prevent any media transfer (Figure 2).

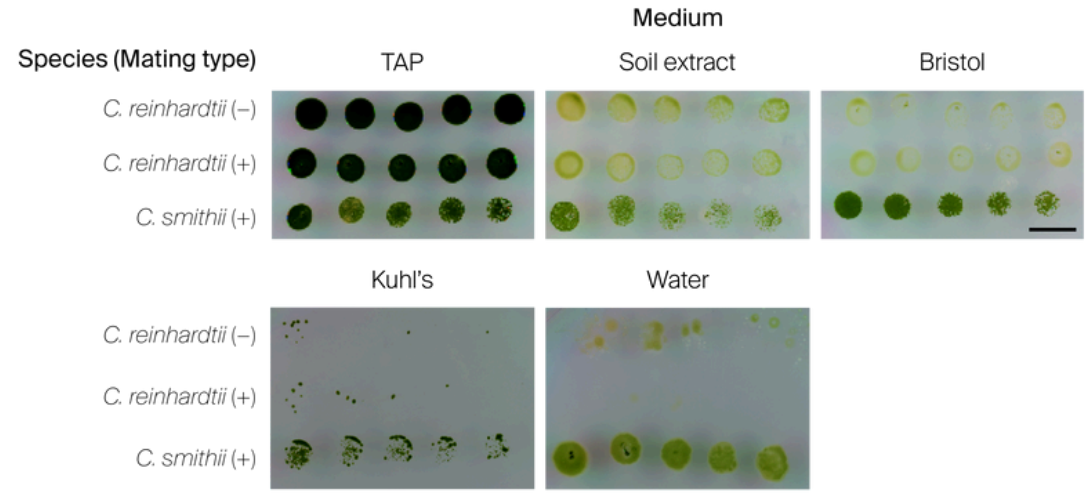

Figure 2. **Both species grow on TAP media, but *Chlamydomonas smithii* can also grow on soil extract media, Bristol media, Kuhl's media, and water**.

Representative spot assays of *C. reinhardtii* (cc-124 and cc-125) and *C. smithii* (cc-1373) on TAP (tris-acetate-phosphate) media, soil extract media, Bristol media, Kuhl's media, or ultrapure water at 24° C under constant illumination for 16 (top row) to 40 days (bottom row) based on the initial cell density. Scale bar: 10 mm.

For additional temperature and light conditions, see Supplemental Figure 1.

Since *C. smithii* was able to grow on rich media that includes ~0.4 mM sodium chloride, we wondered if *C. smithii* could grow on high-salt marine media. We spotted the three *Chlamydomonas* cultures onto different solid marine media that are often used to grow diatoms and other marine protists, which we already had in-house [28][29].

Unsurprisingly, we did not observe any growth on K media, F/2 media, F/2 lacking silica, or synthetic seawater on its own (Figure 3). However, to our surprise, we observed slow, limited growth of *C. smithii* on Erdschreiber's media and on marine broth supplemented with L1 nutrients (MB + L1) (Figure 3). K media and L1 media are very similar except for the tris and ammonium chloride in K media. Since K media was suspended in synthetic seawater and L1 media was suspended in marine broth, we suspected that the peptone, yeast extract, and ferric acid found in marine broth might be responsible for the growth of *C. smithii* on MB + L1 plates, consistent with reports that *C. smithii* shows more heterotrophic growth than *C. reinhardtii* strains [7]. We are currently testing this hypothesis and hope to include the results in future iterations of this pub. Evolutionary studies show some *C. reinhardtii* strains are able to adapt to high-salt conditions and wild marine *Chlamydomonas* species have been isolated [30][31], so it follows that *C. smithii* could survive on marine media, but it's still an intriguing trait that distinguishes the species from our *C. reinhardtii* strains.

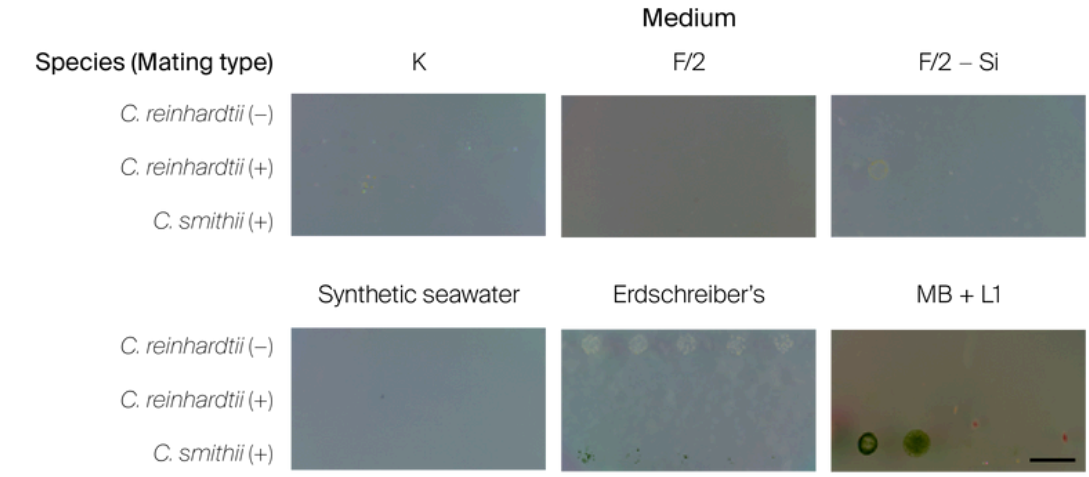

Figure 3. ***C. smithii* can grow slowly on high-salt Erdschreiber's media and marine broth with L1 nutrients included**.

Representative spot assays of *C. reinhardtii* (cc-124 and cc-125) and *C. smithii* (cc-1373) on K media, F/2 media, F/2 media lacking silica, synthetic seawater, Erdschreiber's media, or marine broth (MB) with L1 nutrients, all grown at 24° C under constant illumination for 16–40 days based on initial cell density. Scale bar: 10 mm.

For additional temperature and light conditions, see Supplemental Figure 2.

We've summarized all the *Chlamydomonas* growth patterns we've observed in a graphical table for quick reference (Figure 4).

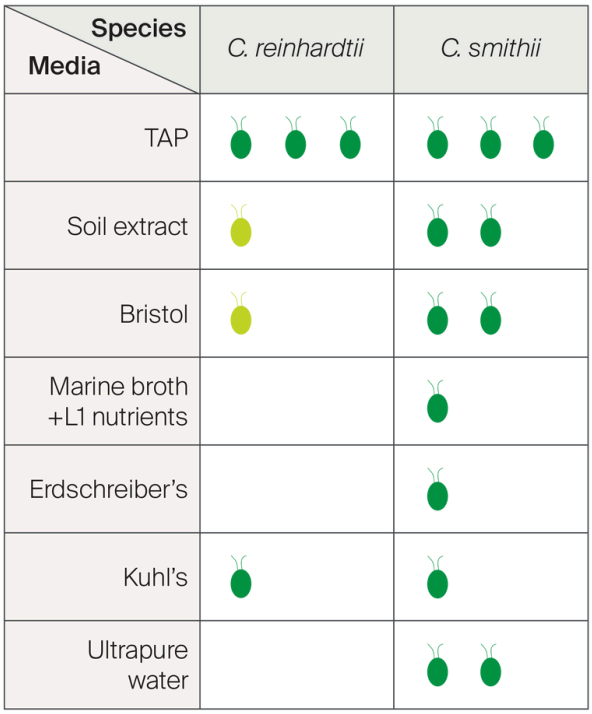

Figure 4. **Visual summary of growth patterns on different types of media**.

The number of *Chlamydomonas* icons indicates qualitative growth rates: 3: fast, 2: medium, 1: slow, 0: none. The color of the cell icon indicates the color of the colonies. The *C. reinhardtii* column represents both strains cc-124 and cc-125.

We did not observe growth on F/2, F/2−Si, K, or synthetic seawater.

Morphological differences after growing on different media

We next took a closer look at single-cell morphology after growth on different types of media. Interestingly, there were no obvious morphological differences between cells grown on fresh water media or Erdschreiber's media. However, cells grown on MB + L1 were larger and either amorphous when suspended in media (Video 1 and Video 2) or swollen when suspended in water (Figure 5).

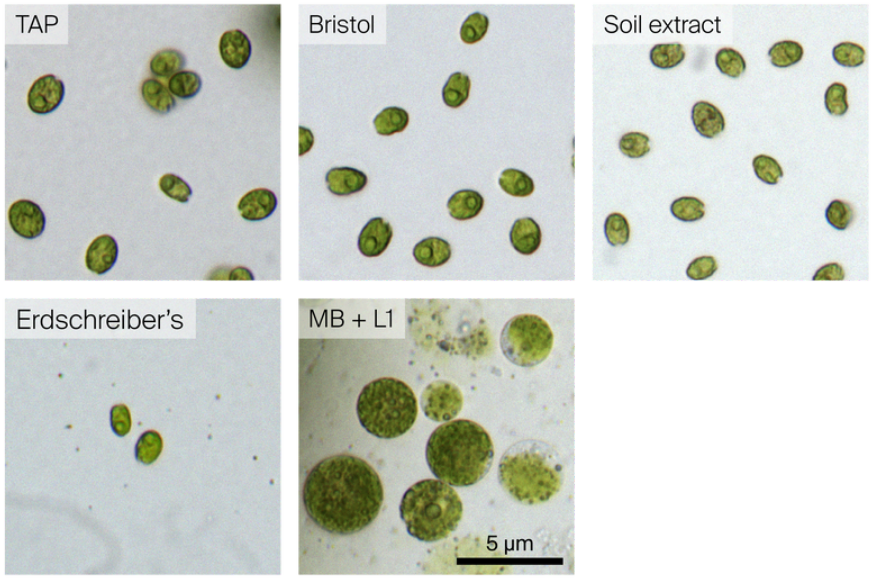

Figure 5. ***C. smithii* cells become large and round on MB + L1 media**.
Representative color images of *C. smithii* grown on the noted media and then resuspended in water for imaging. TAP: tris-acetate-phosphate; MB + L1: marine broth with L1 nutrients added.

When grown on MB + L1 media, we noticed several large *C. smithii* cells with oblong morphologies that quickly rounded up after intense light exposure on the microscope (Video 1). These cells retained their green pigmentation and internal dynamics throughout the experiment, suggesting the cells are alive (Video 2). Surprisingly, we were unable to observe cell division occurring over a 67-hour period. We streaked these cells back onto TAP media and they returned to their normal morphology, confirming that this observation was a result of growth on MB + L1 and not contamination. Because we observed this phenotype in cells grown on MB + L1, but not Erdschreiber's media, we assume the phenotype is not solely salt-induced. *C. reinhardtii* did not grow on any marine media so we did not observe this morphology in either *C. reinhardtii* strain.

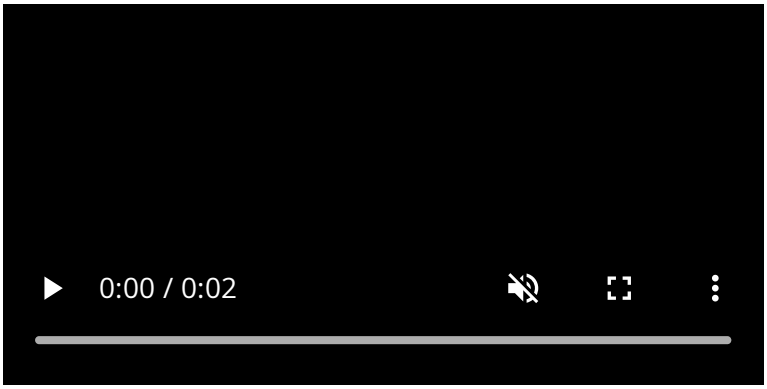

Video 1. ***C. smithii* cells becoming more round upon intense light exposure**.
We grew *Chlamydomonas smithii* cells on 1.5% agar plates supplemented with L1 nutrients and marine broth. We imaged isolates in 400 µm glass wells in L1 media (lacking silica) at 30 minutes/frame.

Video 2. **Amorphous *C. smithii* cells retain healthy color before and after morphological changes**.
We grew *Chlamydomonas smithii* cells on 1.5% agar plates supplemented with L1 nutrients and marine broth. We imaged isolates in 400 µm glass wells in L1 media (lacking silica) at 30 minutes/frame. We captured initial and final frames in RGB, while the intermediate frames were in grayscale.

Sensitivity to detergent

We next compared sensitivity to detergent by treating each strain with 0.05% Triton X-100 to disrupt the cell membrane and release chlorophyll from the cell body. The cell wall can protect the cell membrane from this detergent, preventing lysis from occurring [32]. We collected the lysed cells through centrifugation and quantified the chlorophyll fluorescence in the supernatant as a proxy for total

lysis. We noticed a one-minute treatment with 0.05% Triton X-100 was sufficient to lyse both *C. reinhardtii* and *C. smithii* based on visible green pigment in the supernatant. However, we only observed a statistically significant difference between treated and untreated *C. smithii* samples, while a Kruskal-Wallis test indicated that the difference between treated and untreated *C. reinhardtii* samples was not statistically significant. (Figure 6).

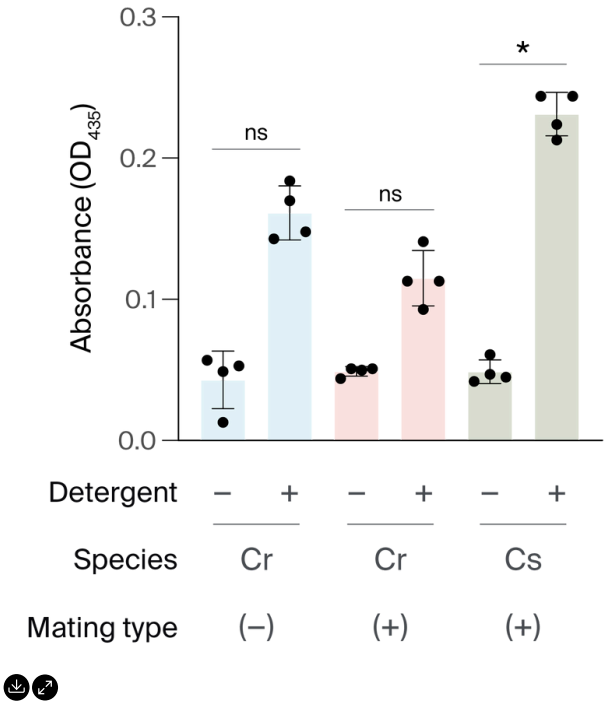

Figure 6. ***C. smithii* is more prone to detergent-induced lysis**.
Bar graph represents the chlorophyll fluorescence in the supernatant of lysed cells after 1 min treatment in 0.05% Triton X-100. Values represent the mean of four reactions. Cr = *C. reinhardtii*; Cs = *C. smithii*. We compared treatments using Kruskal-Wallis ($H = 19.94$, $df = 18$, $p < 0.01$) and Dunn's multiple comparisons test. Asterisks indicate significantly different p values as follows: *$p < 0.05$, ns = not significant.

Morphology

To compare the morphology of the two species, we designed an experiment to collect two-dimensional measurements of motile cells of each species grown on standard TAP media and then suspended in water.

First, we loaded a gamete-enriched population of swimming cells into agar microchambers [19][18]. We selected approximately 30, 100 µm-diameter microchambers for imaging each algal species. Each microchamber contained 1–3

cells. We collected three-minute videos of microchambers at 20 frames per second for subsequent cell morphology analysis. We performed four replicates of the experiment, conducted on different days but with cells obtained from the same lawn plate. Following image acquisition we performed pixel classification in ilastik [23]. We used the ilastik-generated probability maps in CellProfiler [25] to segment cells and generate a data set of 2D morphological measurements (see "Image processing and cell morphology analysis" for more methodological detail and Figure 1 for an overview of our workflow).

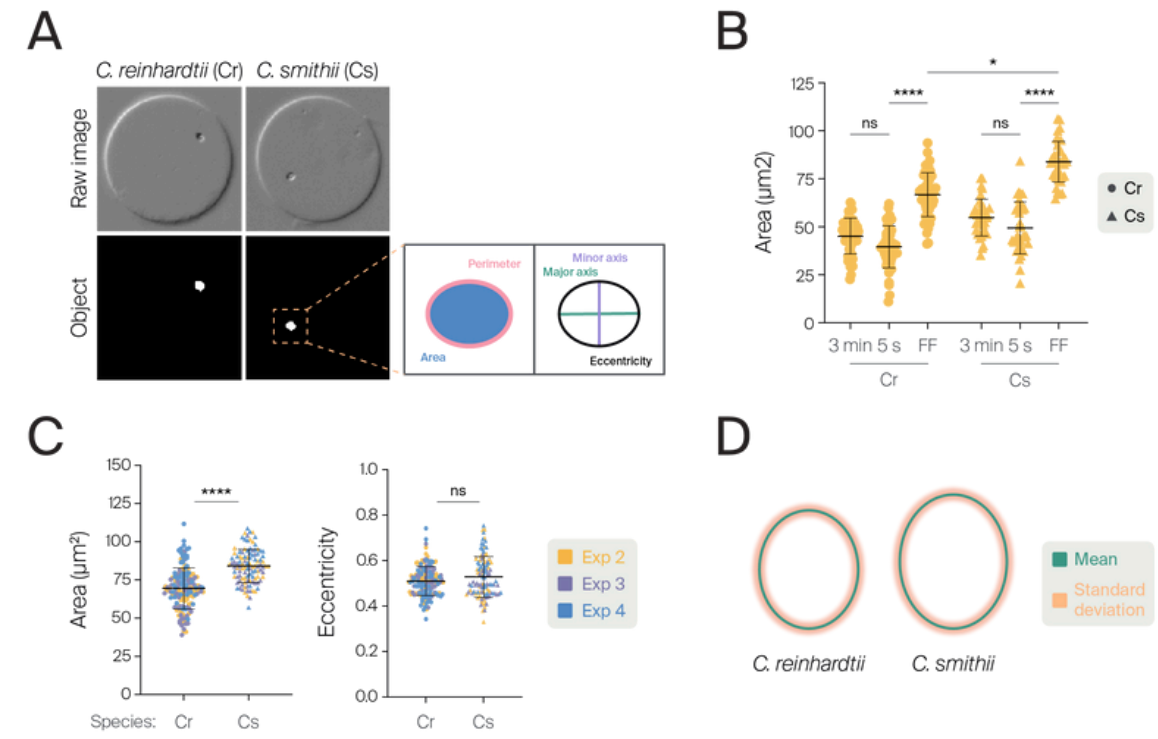

Figure 7. **2D morphological measurements for each species determined from video data of swimming cells**.

(A) Two single frames showing motile *C. reinhardtii* and *C. smithii* cells, each within a 100 µm-diameter agar microchamber. We've diagrammed the morphology measurements that we collected.

(B) Comparison of area measurements for experiment 2 (Exp 2) between the full data set (3 min), a random subset of data (first 5 s), and the focus-filtered (FF) data.

(B–C) Each point in the scatter plot is the mean of measurements from the frames with an object in focus in the video of a single microchamber. We are showing the filtered dataset for experiments 2–4, as we collected these using differential interference contrast (DIC). We compared treatments using a one-way ANOVA ($F(3,129) = 8.229$, $p < 0.0001$) and Dunn's multiple comparisons test. Cr = *C. reinhardtii*; Cs = *C. smithii*. Asterisks indicate significantly different p values as follows: *$p < 0.05$, **$p < 0.01$, and ns = not significant.

(C, left) *C. smithii* has a larger area footprint than *C. reinhardtii* by ~14 μm^2 for each experiment as determined by a Mann-Whitney test, $U = 3241$, $p < 0.0001$. Kruskal-Wallis, $H = 218.8$, $df = 322$, ****$p < 0.0001$.

(C, right) The cell shape (eccentricity) is not statistically different between species as determined by a Mann-Whitney test, $U = 7560$, $p = 0.2247$. However, when we performed a linear regression and controlled for batch effects, there was a statistical difference in eccentricity (see Supplemental Figure 3 for complete data set and linear regression analysis). Horizontal lines indicate the mean, error bars show the standard deviation, ns = not significant.

(D) Drawings represent the average measurements for gametes of each species. Green lines indicate the mean and the orange glow indicates the standard deviation. See Video 3 for a qualitative assessment of the raw data.

In the previous version of this pub, we analyzed all 3,600 frames (3 min) for Experiment 1 (Exp 1) but the processing (training the model in ilastik, generating

probability maps, extracting measurements with CellProfiler) took several days. We also had three other experiments to analyze and so to increase our ability to analyze all four experiments in a timely manner, we used the first 100 frames (5 s). Although this method allowed us to compare five morphology measures between the two species, the first 100 frames were a random subset of the data and included many frames with the cells out of focus. We therefore decided to use a pre-processing filtering step to extract all of the frames where the cell was in focus and select the optimal frames to estimate the morphological characteristics of the cell. To do this, we used a method called "variance of the Laplacian" [24] to determine the edges in a series of images. When we applied this filtering step, we saw that it did not affect the bright-field (BF) data in Exp 1 the same way it worked on the differential interference contrast (DIC) data in Exp 2–4. For this reason, we excluded Exp 1 from our morphology data processing and results. We plan to explore how different filtering approaches work on BF and DIC datasets in an upcoming pub.

For each segmented cell in this set of focus-filtered frames, we measured the area, perimeter, major axis, minor axis, and eccentricity (you can think of this as “roundness”) (Figure 7, A). In the first replicate, we analyzed all 3600 frames of the 3 min videos, but the computational processing time for the analysis was long (many days). To see if we could observe morphology differences with fewer data points, we compared area measurements from the full 3 min videos (3600 frames) with area measurements from the first five seconds of video (100 frames) (Figure 7, B). We decided to analyze the remaining three replicates using five second videos, because the mean area measurements were similar between the 5 s subset and the full 3 min videos, and this decreased computational time for processing all four experiments (Figure 7, C). To explore the data for all five measurements, see Supplemental Figure 3 and Supplemental Table 1.

Supplemental Table 1 - Morphology stats.xlsx Download

We were surprised at the degree of variation we observed for each measure of the population of ~30 cells, as these are clonal cells obtained from the same lawn of growth (Video 3). Additionally, the species type was the most reliable and strongest factor determining differences (Supplemental Figure 3, B), though we did

observe significant variation between experiments (Supplemental Figure 3, C). Both measurements of area and perimeter differed between species across all four experiments, with *C. smithii* being larger. The mean area of *C. smithii* is 69.53 ± 13.44 μm^2, whereas the mean area of *C. reinhardtii* is 84.16 ± 10.85 μm^2 (Figure 7, C and D). The perimeter, as well as the major and minor axes, were all longer in *C. smithii* compared to *C. reinhardtii* (Supplemental Figure 3). However, the eccentricity (a measure of roundness) was similar for both strains (*C. reinhardtii* is 0.51 ± 0.06 compared to 0.53 ± 0.09 for *C. smithii*), but this difference was statistically significant when we performed a linear regression to remove experimental batch effects (Figure 7, C and Supplemental Figure 3).

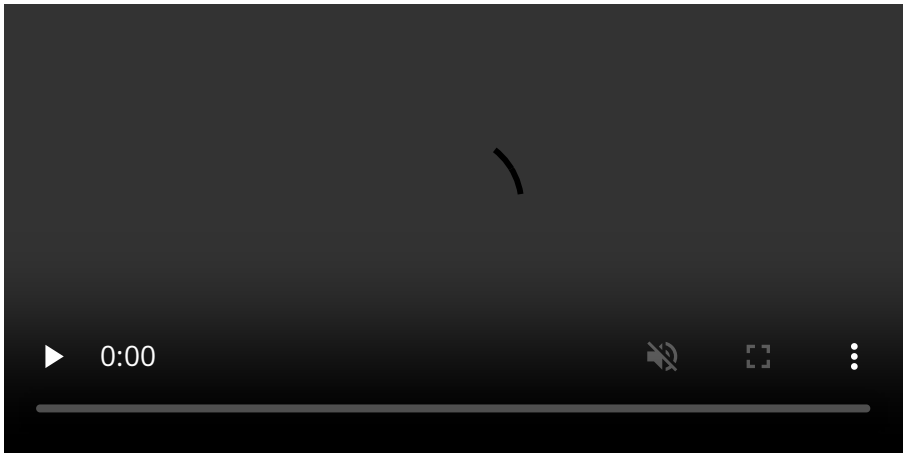

Video 3. **Diversity and mean of 2D morphology measurements of the two species**.
We segmented cells in images and computationally aligned them so that the swimming direction is "up" and the major axis of the cell is coincident with the Y-axis. We're displaying a random subset of cells from three experiments. Cr = *C. reinhardtii*. Cs = *C. smithii*. The "Merge" panel on the right shows cumulative average projections of all the cells, with Cr in magenta and Cs in cyan.

In summary, we found that the gamete form of *C. smithii* is about 14 μm^2 (21%) larger than its *C. reinhardtii* counterpart, but the two species display a similar shape at this life-history stage.

Key takeaways

Chlamydomonas reinhardtii and *smithii* were isolated in the same year under similar conditions and maintained through continuous subculturing, but we have

observed clear differences between the two species:

- *C. smithii* is more adaptable to various growth media ranging from water to nutrient-rich media.
- *C. smithii* takes on a unique morphology when grown on marine broth with L1 nutrients.
- *C. smithii* is more easily lysed in detergent.
- *C. smithii* is 21% larger than *C. reinhardtii*.

Next steps

Our ultimate goal is to find a set of traits that differ quantitatively between *C. reinhardtii* and *C. smithii* so that we can compare the phenotypes of their progeny back to the parent species. We are working to assess other phenotypes in addition to those we have reported here, including organelle morphology (using live, super-resolution fluorescence microscopy), growth curves in liquid media, chloroplast fluorescence decay, individual cell motility behaviors, flagellar beating rates, and phototaxis assays. Please let us know if there are any other phenotypes that you think would be worth exploring!

In addition to identifying useful phenotypes, we're developing novel techniques to quantify them in a high-quality, high-throughput manner. We're also working on high-throughput genotyping methods so that we can thoroughly map genotype-phenotype linkages of the recombinant progeny.

We plan to compare several focus measures to determine which approach is optimal for different types of transmitted light imaging approaches and different levels of sampling resolution and camera detectors. We will assess the approaches on our own bright-field and DIC datasets and integrate open-source datasets (especially if we can find some that also include phase contrast).

We're excited to use this pub as a test case for modular publishing and will continually update the text and figures to reflect new observations and findings, so stay tuned!

Contributors (A–Z)

- **Prachee Avasthi**: Supervision
- **Brae M. Bigge**: Critical Feedback
- **Ben Braverman**: Methodology, Resources
- **Feridun Mert Celebi**: Validation
- **Tara Essock-Burns**: Editing, Formal Analysis, Investigation, Supervision, Visualization
- **Megan L. Hochstrasser**: Editing, Visualization
- **Galo Garcia III**: Formal Analysis, Investigation, Visualization, Writing
- **Cameron Dale MacQuarrie**: Conceptualization, Formal Analysis, Investigation, Visualization, Writing
- **David Q. Matus**: Critical Feedback, Software, Visualization
- **David G. Mets**: Conceptualization, Supervision, Validation
- **Taylor Reiter**: Data Curation, Resources, Validation
- **Harper Wood**: Resources
- **Ryan York**: Conceptualization, Supervision, Visualization, Writing

References

1. Niepoth N, Bendesky A. (2020). How Natural Genetic Variation Shapes Behavior. https://doi.org/10.1146/annurev-genom-111219-080427
2. Bell RA, Cain JR. (1983). Sexual reproduction and hybridization in Chlamydomonas smithii and C. reinhardtii (Chlorophyceae, Volvocales). https://doi.org/10.2216/i0031-8884-22-3-243.1
3. Hoshaw RW, Ettl H. (1966). CHLAMYDOMONAS SMITHII SP. NOV.–A CHLAMYDOMONAD INTERFERTILE WITH CHLAMYDOMONAS REINHARDTIP. https://doi.org/10.1111/j.1529-8817.1966.tb04600.x
4. Harris EH. (2001). CHLAMYDOMONAS AS A MODEL ORGANISM. https://doi.org/10.1146/annurev.arplant.52.1.363
5. Pröschold T, Harris EH, Coleman AW. (2005). Portrait of a Species. https://doi.org/10.1534/genetics.105.044503
6. Harris EH. (1989). An Overview of the Genus Chlamydomonas. https://doi.org/10.1016/b978-0-12-326880-8.50006-7
7. Flowers JM, Hazzouri KM, Pham GM, Rosas U, Bahmani T, Khraiwesh B, Nelson DR, Jijakli K, Abdrabu R, Harris EH, Lefebvre PA, Hom EF, Salehi-Ashtiani K, Purugganan MD. (2015). Whole-Genome Resequencing Reveals

Extensive Natural Variation in the Model Green Alga Chlamydomonas reinhardtii. https://doi.org/10.1105/tpc.15.00492

8. Boynton JE, Harris EH, Burkhart BD, Lamerson PM, Gillham NW. (1987). Transmission of mitochondrial and chloroplast genomes in crosses of Chlamydomonas.. https://doi.org/10.1073/pnas.84.8.2391
9. Nakamura S. (2010). Paternal inheritance of mitochondria in Chlamydomonas. https://doi.org/10.1007/s10265-009-0295-8
10. Colleaux L, Michel-Wolwertz M-R, Matagne RF, Dujon B. (1990). The apocytochrome b gene of Chlamydomonas smithii contains a mobile intron related to both Saccharomyces and Neurospora introns. https://doi.org/10.1007/bf00265065
11. Remacle C, Bovie C, Michel-Wolwertz M-R, Loppes R, Matagne RF. (1990). Mitochondrial genome transmission in Chlamydomonas diploids obtained by sexual crosses and artificial fusions: Role of the mating type and of a 1 kb intron. https://doi.org/10.1007/bf00265051
12. Buchberger F, Stibor H, Neusius D, Nickelsen J, Stockenreiter M. (2019). Transgenic and cell wall-deficient Chlamydomonas reinhardtii food affects life history of Daphnia magna. https://doi.org/10.1007/s10811-019-01983-7
13. Rochaix J-D. (2013). Chlamydomonas reinhardtii. https://doi.org/10.1016/b978-0-12-374984-0.00230-8
14. https://automeris.io/webplotdigitizer
15. JONES GE. (1967). PRECIPITATES FROM AUTOCLAVED SEAWATER1. https://doi.org/10.4319/lo.1967.12.1.0165
16. https://elischolar.library.yale.edu/cgi/viewcontent.cgi?article=1581&context=journal_of_marine_research
17. Avasthi P, Essock-Burns T, Garcia III G, Gehring J, Matus DQ, Mets DG, York R. (2023). Gotta catch ‘em all: Agar microchambers for high-throughput single-cell live imaging. https://doi.org/10.57844/arcadia-v1bg-6b60
18. Essock-Burns T. (2023). Molding microchambers in agar with PDMS stamps for live imaging v1. https://doi.org/10.17504/protocols.io.j8nlkwpk1l5r/v1
19. Thevenaz P, Ruttimann U, Unser M. (1998). A pyramid approach to subpixel registration based on intensity. https://doi.org/10.1109/83.650848
20. Bentley SA, Anagnostidis V, Schlogelhofer HL, Gielen F, Wan KY. (2021). Phenotyping single-cell motility in microfluidic confinement.

https://doi.org/10.1101/2021.12.24.474109

21. Schindelin J, Arganda-Carreras I, Frise E, Kaynig V, Longair M, Pietzsch T, Preibisch S, Rueden C, Saalfeld S, Schmid B, Tinevez J-Y, White DJ, Hartenstein V, Eliceiri K, Tomancak P, Cardona A. (2012). Fiji: an open-source platform for biological-image analysis. https://doi.org/10.1038/nmeth.2019
22. Berg S, Kutra D, Kroeger T, Straehle CN, Kausler BX, Haubold C, Schiegg M, Ales J, Beier T, Rudy M, Eren K, Cervantes JI, Xu B, Beuttenmueller F, Wolny A, Zhang C, Koethe U, Hamprecht FA, Kreshuk A. (2019). ilastik: interactive machine learning for (bio)image analysis. https://doi.org/10.1038/s41592-019-0582-9
23. Salido J, Sánchez C, Ruiz-Santaquiteria J, Cristóbal G, Blanco S, Bueno G. (2020). A Low-Cost Automated Digital Microscopy Platform for Automatic Identification of Diatoms. https://doi.org/10.3390/app10176033
24. Stirling DR, Swain-Bowden MJ, Lucas AM, Carpenter AE, Cimini BA, Goodman A. (2021). CellProfiler 4: improvements in speed, utility and usability. https://doi.org/10.1186/s12859-021-04344-9
25. Glaesener AG, Merchant SS, Blaby-Haas CE. (2013). Iron economy in Chlamydomonas reinhardtii. https://doi.org/10.3389/fpls.2013.00337
26. Vítová M, Bišová K, Hlavová M, Kawano S, Zachleder V, Čížková M. (2011). Chlamydomonas reinhardtii: duration of its cell cycle and phases at growth rates affected by temperature. https://doi.org/10.1007/s00425-011-1427-7
27. Guillard RRL. (1975). Culture of Phytoplankton for Feeding Marine Invertebrates. https://doi.org/10.1007/978-1-4615-8714-9_3
28. Keller MD, Selvin RC, Claus W, Guillard RRL. (1987). MEDIA FOR THE CULTURE OF OCEANIC ULTRAPHYTOPLANKTON[1,2]. https://doi.org/10.1111/j.1529-8817.1987.tb04217.x
29. Shetty P, Gitau MM, Maróti G. (2019). Salinity Stress Responses and Adaptation Mechanisms in Eukaryotic Green Microalgae. https://doi.org/10.3390/cells8121657
30. Hellebust JA, Le Gresley SML. (1985). Growth characteristics of the marine rock pool flagellate Chlamydomonas pulsatilla Wollenweber (Chlorophyta). https://doi.org/10.2216/i0031-8884-24-2-225.1
31. Hwang H-J, Kim Y, Kang N, Han J. (2018). A Simple Method for Removal of the Chlamydomonas reinhardtii Cell Wall Using a Commercially Available Subtilisin (Alcalase). https://doi.org/10.1159/000495183